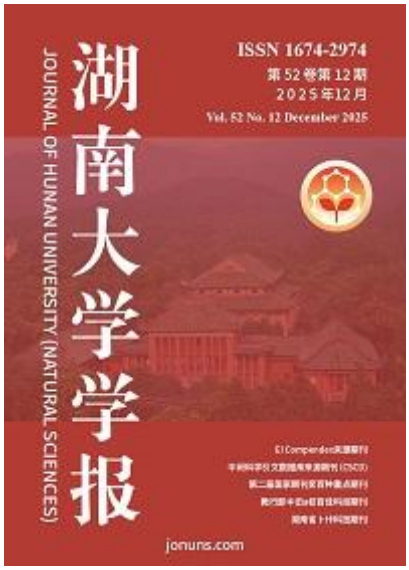

Journal of Hunan University

(Natural Sciences)

Vol. 52 No. 12

December 2025

Available online at

https://jonuns.com

Open Access Article

https://doi.org/10.55463/issn.1674-2974.52.12.14

Adaptation of The Eligehausen Model to Experimental Results of Shear Stress at The Steel-Cement Mortar Interface Tests

Azdine Ilhame[1,*], Kissi Benaissa[2], Khatib Hamza[2]

[1] Department of Physics and Applications, Faculty of Sciences Ben M'sick, Hassan II University, Casablanca 20670, Morocco,

[2] Systèmes Cyber Physiques Complexes (CCPS), National School of Arts and Crafts, Hassan II University, Casablanca 20670, Morocco,

* Corresponding author: Ilhame.azdine@gmail.com

Article history
Received: November 21, 2025
Revised: December 29, 2025
Accepted: January 8, 2026
Published: January 30, 2026

Abstract: This paper presents an adapted version of the Eligehausen bond–slip model aimed at more accurately reproducing the mechanical response of ribbed steel–cement mortar interfaces observed in direct shear tests reported in previous studies. The proposed approach introduces a refined analytical formulation that overcomes key limitations of existing bond–slip laws, particularly their inability to adequately describe the nonlinear adhesion and slip behavior characteristic of steel–mortar composite interfaces.

The objective of this research is to develop a constitutive law that more reliably characterizes the shear stress–slip relationship and reflects the actual adhesion mechanisms identified experimentally. A series of direct shear tests was conducted on high-strength cement mortar cast between two steel plates. The resulting stress–deformation curves were analyzed to identify the governing parameters of the interfacial bond mechanism.

The Eligehausen model was implemented and calibrated using MATLAB through an iterative optimization procedure designed to minimize discrepancies between experimental and analytical results. The calibrated model demonstrates a significantly improved agreement with the experimental stress–slip responses compared to the original formulation. In particular, it successfully captures both the nonlinear ascending branch and the subsequent softening behavior, which are not adequately represented by existing models.

The study introduces modified equations that enhance the physical interpretation of adhesion and frictional mechanisms at the steel–mortar interface. The proposed constitutive model provides a more accurate description of shear loading behavior and enables more reliable numerical simulations of steel–mortar composite connections.

Keywords: Steel–cement mortar interface; Bond–slip behavior; Adhesion mechanisms; Direct shear test; Constitutive modeling.

钢—水泥砂浆界面剪切应力试验实验结果下 Eligehausen 模型的适应性研究

摘要：本文提出了一种改进的 Eligehausen 粘结–滑移模型，旨在更准确地再现先前研究中直接剪切试验所观测到的带肋钢筋—水泥砂浆界面的力学响应。该研究提出了一种精细化的解析模型，克服了现有粘结–滑移本构关系的主要局限性，尤其是其难以合理描述钢—砂浆复合界面中非线性粘结与滑移行为的问题。

本研究的目标是建立一种能够更可靠表征剪切荷载作用下应力–滑移关系的本构模型，并真实反映实验中观察到的界面粘结机理。为此，在两块钢板之间浇筑高强度水泥砂浆并开展了一系列直接剪切试验，对所得的应力–变形曲线进行了分析，以确定界面粘结机制的控制参数。

采用 MATLAB 实现并标定 Eligehausen 模型，通过迭代优化方法最小化实验结果与理论预测之间的差异。标定后的模型与实验应力–滑移曲线表现出显著提高的一致性，尤其能够准确捕捉非线性上升段及随后的软化行为，而这些特征在现有模型中通常难以充分描述。

本研究引入了修正方程，从而增强了对钢—水泥砂浆界面粘结与摩擦机理的物理解释能力。所提出的本构模型能够更准确地描述剪切荷载条件下的界面行为，并为钢—砂浆复合连接的数值模拟提供更可靠的理论基础。

关键词：钢—水泥砂浆界面；粘结–滑移行为；粘结机理；直接剪切试验；本构建模

1. Introduction

Steel-concrete composite bridges are a category of structures widely used in modern engineering structures due to their mechanical efficiency and durability. They are primarily loaded in bending and consist of steel and concrete elements connected by shear connectors that ensure the continuity of force transfer at the interface. These connectors prevent both relative slippage and separation between the materials, thus ensuring fully composite behavior. A well-designed shear connection allows the steel and concrete to work together as a single structural element, forming a composite beam capable of effectively resisting service and extreme loads. [1-2-3]

The proper functioning of these structures depends heavily on the quality of the interface between steel and concrete. This interface, subject mainly to shear stresses, ensures adhesion and the transfer of forces between the two materials. The characterization of this interaction zone is therefore essential to understand the phenomena of sliding, cracking and detachment likely to alter the overall performance of the structure. Recent experimental research, based on push-out or direct traction tests, has highlighted the complex nature of stress-slip behavior and refined the analytical models describing the steel-concrete bond. [4-5-6]

The bond behavior between steel and cement grout material plays a crucial role in the performance of composite structures, influencing their load transfer efficiency and overall mechanical behavior. Understanding this interaction is essential for improving the reliability and durability of steel–concrete and steel–mortar connections. In recent decades, several studies have investigated the mechanisms governing the bond–slip relationship in reinforced and composite materials,

leading to the development of analytical and empirical models. [7]

Among them, the Eligehausen model has been widely recognized for its ability to describe the nonlinear bond–slip behavior observed in ribbed steel–concrete interfaces. However, when applied to high-strength mortar or modified interface geometries, this model often fails to accurately reproduce experimental responses due to its simplified assumptions regarding adhesion and frictional behavior. [8-9]

To address these limitations, the present study proposes an adapted version of the Eligehausen bond model specifically tailored to steel–cement mortar interfaces. The model aims to capture the nonlinear adhesion and slip characteristics revealed through direct shear tests performed on high-strength mortar poured between steel plates. [10]

A series of experimental investigations was conducted to identify the governing parameters of the bond mechanism, has been used to implement and calibrate the analytical model, MATLAB software has been used to minimize discrepancies between experimental and numerical results.

2. Presentation of Experimental Results

The experimental results presented in Figure 1 highlight the bond stress behavior as a function of deformation of the OR2 subjected to a high confining stress. This result demonstrates a high-strength bond, illustrated by a characteristic curve comprising a nonlinear ascending phase, a plateau corresponding to the maximum bond stress, followed by a decrease towards a residual stress. These different phases reflect the complex adhesion and sliding phenomena at the steel–concrete interface, including the progressive activation of load transfer mechanisms. The analysis of these results provides a better understanding of the local behavior of the interface. [10].

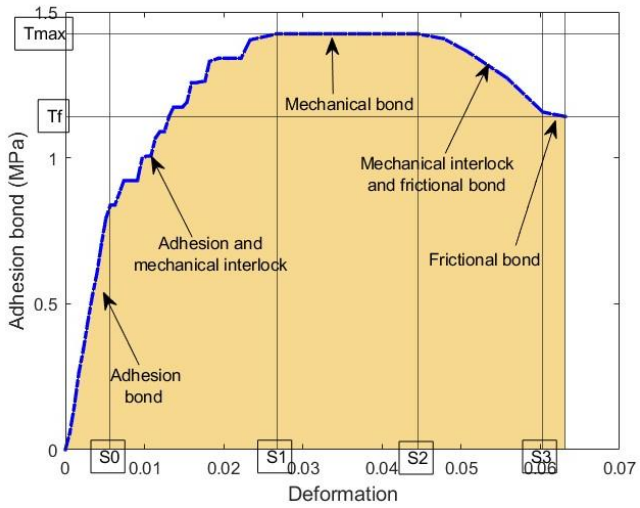

Figure 1. Characteristic of the adhesion stress of the OR2 specimen "Developed by the authors".

Before proceeding with the adaptation of the model, it is essential to recall the main characteristics of the experimental results obtained. The adhesion stress-deformation curves present the following phases:

Quasi-linear initial phase ($0 - S_0$)*:* A rapid increase in the bond stress with deformation, suggesting a behavior dominated by chemical adhesion and friction [11]. This phase ends at the point (S_0, τ_0), where S_0 represents the slip at the beginning of the nonlinear phase and τ_0 the corresponding bond stress.

Nonlinear phase ($S_0 - S_1$)*:* A transition to nonlinear behavior, where the bond stress continues to increase, but at a decreasing rate. This phase is influenced by the mechanical interaction of the ribs with the cement mortar.

Maximum adhesion stress phase ($S_1 - S_2$)*:* Reaching a maximum adhesion stress (τ_{max}), followed by a pronounced plateau.

Degradation phase ($S_2 - S_3$)*:* Progressive decrease in adhesion stress due to damage and rupture of the interface.

Residual phase ($S > S_3$)*:* Stabilization of the adhesion stress at a residual value (τ_f), representing the residual friction between the steel and the mortar.

These experimental observations highlight the complexity of the interface behavior and the need for a model capable of capturing these different phases. [12]

3. Adaptation of the Eligehausen Model: Challenges and Approaches

3.1. Reminder of the Eligehausen Model

The original Eligehausen [13-14] model presented in **Figure *2*** is defined by the following equations:

initial phase ($0 \leq S \leq S_1$):

$$\tau = \tau_{max} \times (\frac{S}{S_1})^{\alpha} \quad (1)$$

Maximum adhesion stress phase ($S_1 < S \leq S_2$):

$$\tau = \tau_{max} \quad (2)$$

Degradation phase ($S_2 < S \leq S_3$):

$$\tau = \tau_{max} - \frac{\tau_{max} - \tau_f}{S_2 - S_3} \times (S - S_2) \quad (3)$$

Residual phase ($S > S_3$):

$$\tau = \tau_f \quad (4)$$

The analysis of the experimental results made it

possible to identify the key points of the model's behavior: τ_{max} and τ_f : Maximum adhesion stress reached and residual stress, are directly extracted from the experimental curves.

S_1, S_2, S_3: Slip values corresponding to the transitions between the different phases of the model, are identified at the points of change in the slope of the curve.

α is a curvature adjustment parameter, to be adjusted using an optimization method to minimize the error between the model and the experimental data.

The experimental curves show a good correspondence with the theoretical phases of the model, but adjustments are necessary to faithfully reflect reality.

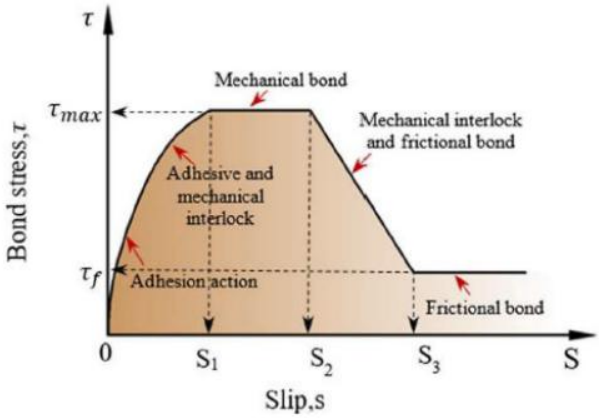

Figure 2. Eligehausen model [13].

3.2. Preliminary Results: Application of the Original Model

To assess the fit of the Eligehausen model to our experimental results, we directly applied the power law over the entire interval $[0, S_1]$. The parameter α was optimized to minimize the error between the experimental curves and those produced by the model.

3.2.1. Methodology

The parameter α was optimized by minimizing the sum of squared errors (SSE) between the experimental data and the model predictions. The objective function is defined as follows:

$$SSE = \sum_{i=1}^{n} (\tau_{exp,i} - \tau_{model,i})^2 \quad (5)$$

Where:

n is the number of experimental points in the interval $[0, S_1]$.

$\tau_{exp,i}$ is the experimental stress at point i.

$\tau_{model,i}$ is the stress predicted by the model at point i, given by:

$$\tau_{model,i} = \tau_{max} \times (\frac{S_i}{S_1})^{\alpha} \quad (6)$$

3.2.2. Results

Figure 2 compares the experimental curves with those produced by the Eligehausen model over the interval $[0, S_1]$, estimating the optimal value of αinitial at 0.46338.

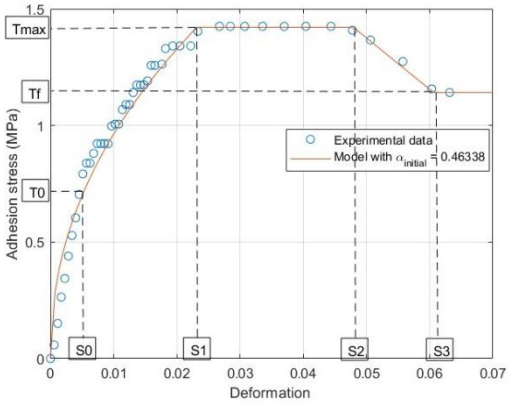

Figure 3. Eligehausen Model (Initial Alpha: 0.46338) "Developed by the authors".

3.2.3. Interpretation of Results

The results show that, although the Eligehausen model can approximately capture the general trend of the data in the interval $[0, S_1]$, it does not faithfully reproduce the quasi-linear initial phase observed experimentally between 0 and S_0. Indeed:

- The original model does not faithfully capture the quasi-linear initial phase.
- The power law imposes a curvature from the beginning, which does not correspond to the linear behavior observed experimentally.
- The error is particularly significant in the region close to 0, where the model systematically overestimates or underestimates the experimental values.

These observations highlight a fundamental limitation of the original model when applied to our data.

3.3. Introduction of a Linear Solution for the Initial Phase

To better represent the experimentally observed quasi-linear initial phase, a linear relationship was introduced for slips between 0 and S_0. The proposed modification is defined as follows:

3.3.1. Modified Model

Linear phase ($0 \leq S \leq S_0$):

$$\tau = \frac{S}{S_0} \times \tau_0 \quad (7)$$

Where:
$S_0 = 0.00512045$ mm
$\tau_0 = 0.792132$ MPa

Nonlinear phase (S0 < S ≤ S1):

The original power law of the Eligehausen model is preserved:

$$\tau_{model,i} = \tau_{max} \times (\frac{S_i}{S_1})^{\alpha} \quad (8)$$

The other phases ($S_1 < S \leq S_2$, $S_2 < S \leq S_3$, $S > S_3$) remain unchanged.

3.4. Results with the Linear Solution

Figure *4* compares the experimental curves with those produced by this modified model.

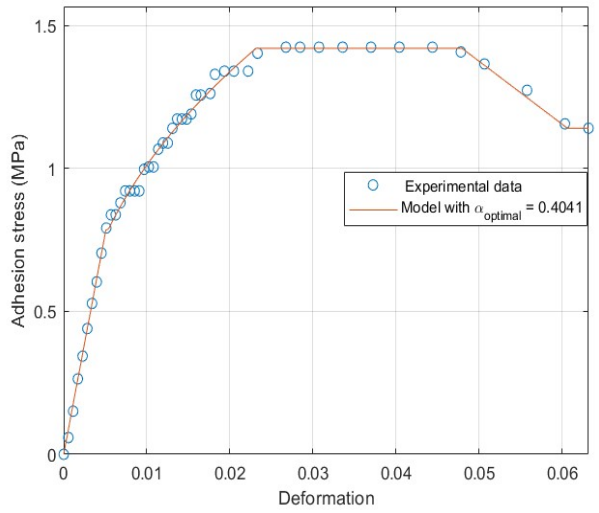

Figure 4. Model with Linear Phase (Optimal Alpha: 0.4041 "Developed by the authors".

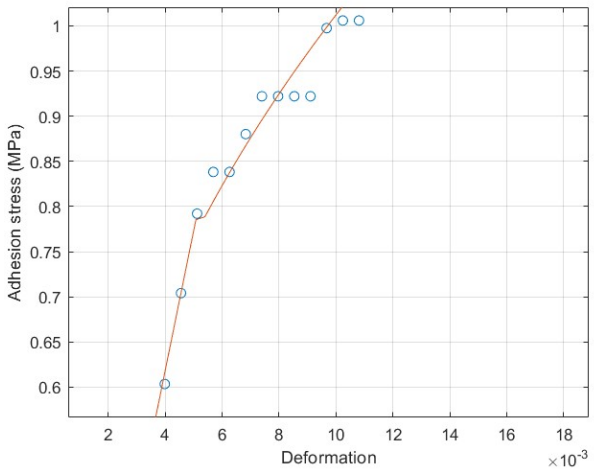

Figure 5. Discontinuity "Developed by the authors".

3.5. Interpretation of Results

The introduction of a linear phase better represents the quasi-linear behavior observed experimentally between 0 and S_0. However, this modification introduces a discontinuity at the point (S_0, τ_0), because there is no smooth transition between the linear part and the power law.

The results obtained are shown in figure 4.

These challenges highlight the limitations of the original model and motivate the adaptations proposed in the following sections to better represent our experimental data while respecting the physical constraints of the problem.

3.5.1. Correction of the Discontinuity at Point (S_0, τ_0)

To eliminate the discontinuity at point ((S_0, τ_0), the power law used in the interval $[S_0, S_1]$ was modified to ensure continuity at point (S_0, τ_0). In addition, the parameter α was locally optimized to minimize the discrepancy between the model and the experimental data.

$$\tau = \tau_0 + (\tau_{max} - \tau_0) \times \frac{S - S_0}{S_1 - S_0}, 0 \leq S \leq S_1 \quad (9)$$

The parameter α was optimized by minimizing the sum of squared errors (SSE) over the interval $[S_0, S_1]$. The optimization yielded a new optimal value $\alpha_{optimal} = 0.79648$.

Figure *7* shows the experimental curves compared to the corrected model with continuity at point (S_0, τ_0).

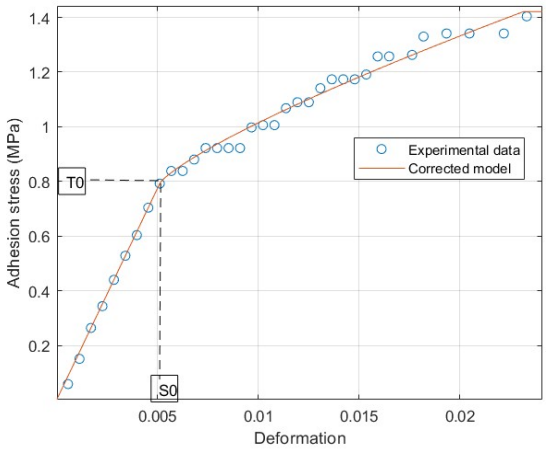

Figure 6. Model with Continuity (Optimal Alpha: 0.79648) "Developed by the authors".

3.5.2. Analysis and Discussion

The correction made to the power law allows us to completely eliminate the discontinuity at point (S_0, τ_0) while maintaining a smooth transition between the linear and nonlinear phases:

- Mathematical continuity is respected.
- The overall behavior of the model is consistent with experimental observations.

3.6. Correction of the Curve over the Interval [S2, S3]

3.6.1. Problem

In the original Eligehausen model, the descending phase between S_2 and S_3 is represented by a linear curve. However, our experimental data show that this decay is not always linear and can have a more complex shape.

3.6.2. Methodology

To better represent the degradation phase, the assumption of a linear decay was replaced by a decreasing exponential function. This approach is motivated by the experimental observation of a smoother transition between the plateau phase and the degradation phase. The new equation for the interval $[S_2, S_3]$ is:

$$\tau = \tau_f + (\tau_{max} - \tau_f) \times \left(1 - \left(\frac{S - S_2}{S_3 - S_2}\right)^{\beta}\right) \quad (10)$$

where β is a new parameter to optimize that controls the decay of the curve.

We optimized the parameter β (for the degradation phase) using the least squares method over the interval $[S_2, S_3]$. The optimization set the optimal value of $\beta_{optimal}$ to 1.4092 .

3.7. Results

Figure *7* shows the comparison between the experimental data and the final model, including all modifications made.

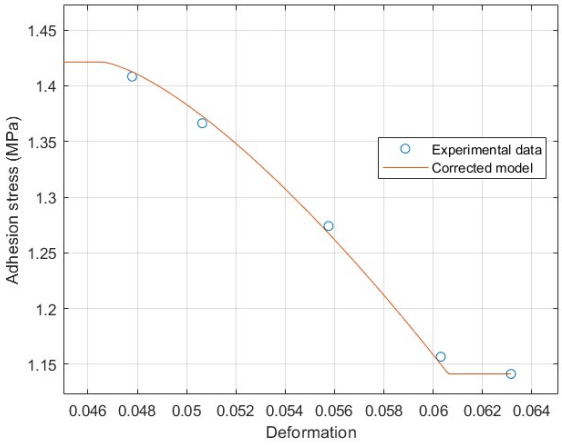

Figure 7. Corrected model with (Beta optimal: 1.4092) "Developed by the authors".

This modification, combined with the previous ones, makes it possible to obtain a more faithful model over the entire deformation range, from the initial phase to the residual phase.

$$\tau = \begin{cases} \frac{\tau_0}{S_0} \times S & for \ \ S \le S_0 \\ \tau_0 + (\tau_{max} - \tau_0) \times \frac{S - S_0}{S_1 - S_0} & for\ S_0 < S \le S \\ \tau_{max} & for\ S_1 < S \le S \\ \tau_f + (\tau_{max} - \tau_f) \times \left(1 - \left(\frac{S - S_2}{S_3 - S_2}\right)^{\beta}\right) & for\ S_2 < \\ \tau_f & for\ S > S_3 \end{cases} \quad (11)$$

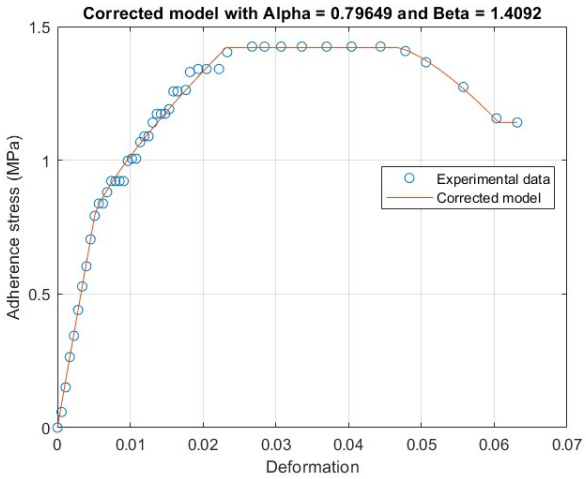

Figure 8. New model adapted to the steel-cement mortar interface "Developed by the authors".

4. Model Performance Evaluation

The performance of the corrected model was quantitatively evaluated using two commonly used statistical indicators: the root mean square error ($RMSE$) and the coefficient of determination (R^2).

4.1. Root Mean Square Error (RMSE)

The root mean square error (RMSE) measures the average deviation between the values predicted by the model and the values observed experimentally. It is defined as follows:

$$RMSE = \sqrt{\frac{1}{n}\sum_{i=1}^{n}(\tau_{exp,i} - \tau_{model,i})^2} \quad (12)$$

Where:

n is the number of data points,

$\tau_{exp,i}$ is the experimentally measured adhesion stress at point i,

$\tau_{model,i}$ is the adhesion stress predicted by the model at point i.

A low RMSE value indicates good model accuracy.

4.2. Coefficient of Determination (R^2)

The coefficient of determination (R^2) measures the proportion of the total variance in experimental data that is explained by the model. It is defined as follows:

$$R^2 = 1 - \frac{\sum_{i=1}^{n}(\tau_{exp,i} - \tau_{model,i})^2}{\sum_{i=1}^{n}(\tau_{exp,i} - \bar{\tau}_{exp})^2} \quad (13)$$

Where:
$\bar{\tau}_{exp}$ is the average of the experimental adhesion stresses.

The R^2 varies between 0 and 1, where a value close to 1 indicates an excellent fit of the model to the data.

4.3. Results Evaluation

By applying these statistical indicators to our corrected model, we obtain the following results:

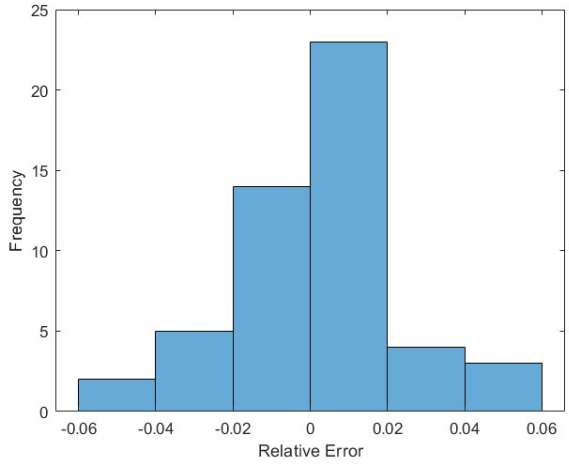

Figure 9. Model Error Distribution "Developed by the authors".

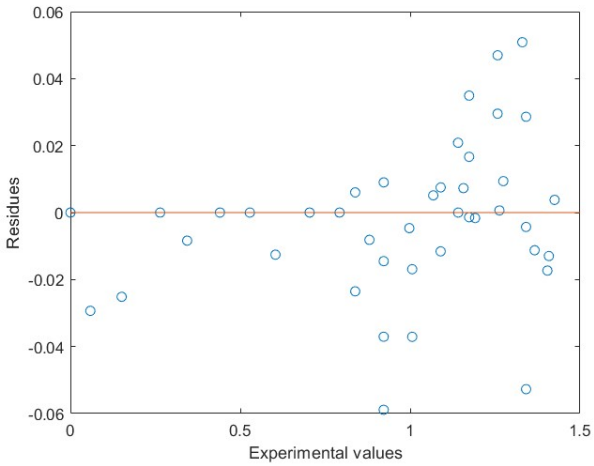

Figure 10. Residuals graph "Developed by the authors".

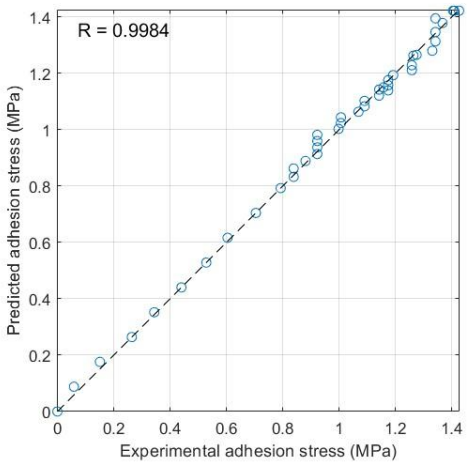

Figure 11. Correlation between experimental and predicted values "Developed by the authors".

4.4. Analysis and Discussion

The results obtained demonstrate the remarkable performance of the developed model for predicting steel-concrete bond behavior. The high R^2 correlation coefficient, reaching 0.9984 , demonstrates excellent agreement between model predictions and experimental observations. This strong correlation indicates that the model accurately captures the fundamental mechanisms governing bond strength in this composite system.

Analysis of the error distribution reveals a distribution centered around zero, suggesting the absence of systematic biases in the model's predictions. This observation is crucial, as it confirms that the model neither predictably overestimates nor underestimates adhesion stress values. The error histogram confirms this conclusion, showing a concentration of errors

around the zero value, indicating good overall model accuracy.

Detailed examination of the residuals reveals a remarkable overall performance of the model over the entire bond stress range studied. The slight increase in residual dispersion observed for higher bond stress values deserves special attention. This observation could reflect the increasing complexity of steel-concrete interactions at higher stress levels. It also highlights the model's ability to capture nuances of bond behavior, even under more demanding conditions. These results open interesting perspectives for future research, particularly in the deeper exploration of high-stress bond mechanisms. The current model thus provides a solid basis for further developments, providing a valuable tool for the design and analysis of bonded connections, while identifying avenues of investigation to further refine our understanding of this complex phenomenon.

5. Conclusion

This study developed an adapted version of the Eligehausen bond–slip model to more accurately reproduce the mechanical behavior of ribbed steel–cement mortar interfaces under direct shear loading. The refined formulation successfully captured the nonlinear ascending branch, peak adhesion strength, and progressive post-peak softening observed experimentally. Model calibration using MATLAB significantly reduced the discrepancies between analytical predictions and experimental stress–slip curves, demonstrating the improved accuracy and robustness of the proposed approach.

Rigorous evaluation of the model's performance, using statistical indicators such as root mean square error $RMSE$ and coefficient of determination R^2, demonstrated its high accuracy. The correlation coefficient R^2 of 0.9984 testifies to the excellent ability of the model to predict adhesion behavior over the entire stress range studied.

Compared to earlier models in the literature, including the original Eligehausen formulation, the proposed adaptation offers superior predictive performance for high-strength mortar interfaces. While traditional models generally assume simplified adhesion and friction mechanisms, the refined model allows a more realistic representation of the shear transfer process.

In conclusion, this work provides a valuable tool for understanding and predicting the behavior of steel-cement mortar bond. The developed model provides a solid basis for the design and analysis of reinforced concrete structures, while opening new perspectives for future research in this crucial area of structural engineering. Future studies could explore the applicability of this adapted model to a broader range of interface conditions, including different mortar strengths, surface geometries, and loading scenarios. Incorporating the model into full-scale numerical simulations would further validate its performance in realistic structural configurations.

Declarations

Author Contributions

Conceptualization, methodology, software, investigation, resources, writing—original draft preparation I.A.; validation, writing—review and editing, visualization, supervision, K.B. and K.H.; All authors have read and agreed to the published version of the manuscript.

References

[1] YANG D., LI G., ZHANG J., YUAN Y., AU F.T.K. *Shear connector performance analysis for composite corrugated steel–concrete bridge decks.* Journal of Constructional Steel Research, Elsevier, (2025).
[2] ZHANG C., HUANG W., LIU Y., LI S. *Experimental study on mechanical performance of corrugated steel–concrete composite bridge decks under positive and negative bending moments.* Scientific Reports – Nature Publishing Group. (2025).
[3] WANG J., CHEN X., GUO F., XU Y. *Shear behavior of prefabricated steel–concrete connectors with improved bond-slip characteristics.* Scientific Reports, Nature. (2024).
[4] WANG, K., & ZHANG, H. I*nterfacial shear behavior in steel–concrete–steel composite slabs under cyclic loading.* Engineering Structures.(2023).
[5] THOMANN, M. *Connexions par adhérence pour les ponts mixtes acier–béton.* EPFL Thèse. (2025).
[6] ZHANG, C., HUANG, W., LIU, Y. *Experimental investigation of bond behavior in composite bridge girders.* Engineering Structures. (2024).
[7] H. YUAN AND H. BING. *Experimental study on bond behavior between high-strength grout and deformed steel bars.* Construction and Building Materials, 301:124059, 2021.
[8] I. AZDINE, B. KISSI, AND H. KHATIB. *Study of direct shear of the adhesion connectors steel-concrete.* In 2nd International Conference on Innovative Research in Applied Science, Engineering and Technology (IRASET), pages 1–4, Meknes, Morocco, 2022.
[9] I. Azdine, B. Kissi, H. Khatib, and A. Ziraoui. *Analysis of the shear stress at the interface between steel and cement grout.* Materials Today: Proceedings, 2025.
[10] ILHAME, A., BENAISSA, K., HAMZA, K., ADIL, Z., MARIA, E. *Experimental study on the behavior of cement grout-steel sheet interface under shear forces.* Journal of

Building Pathology and Rehabilitation 10, 52 (2025).
[11] WILLIAMS PAUCHET. *Adherence acier-beton.* Techniques de l'Ingenieur, 2024.
[12] ANTOINE TIXIER. A*nalyse du comportement de l'interface acier-béton par essai push-in : Mesures par fibres optiques et modélisation par éléments finis.* Thèse de doctorat, Université de Grenoble, 2013.
[13] R. ELIGEHAUSEN, E. P. POPOV, AND V. V. BERTERO. *Local bond stress-slip relationships of deformed bars under generalized excitations.* Report No. UCB/EERC-83/23, October 1983.
[14] H. LIN, Y. ZHAO, J. OZBOLT, P. FENG, C. JIANG, AND R. ELIGEHAUSEN. *Analytical model for the bond stress-slip relationship of deformed bars in normal strength concrete.* Construction and Building Materials, 198:570–586, 2019.

参考文:

[1] YANG D., LI G., ZHANG J., YUAN Y., AU F.T.K.
波纹钢—混凝土组合桥面板剪力连接件性能分析。*Journal of Constructional Steel Research*, Elsevier, （2025）。
[2] ZHANG C., HUANG W., LIU Y., LI S.
正负弯矩作用下波纹钢—混凝土组合桥面板力学性能的试验研究。*Scientific Reports*, Nature Publishing Group, （2025）。
[3] WANG J., CHEN X., GUO F., XU Y.
具有改进粘结–滑移特性的预制钢—混凝土连接件剪切性能研究。*Scientific Reports*, Nature, （2024）。
[4] WANG K., ZHANG H.
循环荷载作用下钢—混凝土—钢组合板的界面剪切行为。*Engineering Structures*, （2023）。
[5] THOMANN M.
钢—混凝土组合桥梁中的粘结连接。EPFL 博士论文, （2025）。
[6] ZHANG C., HUANG W., LIU Y.
组合桥梁主梁中界面粘结行为的试验研究。*Engineering Structures*, （2024）。
[7] YUAN H., BING H.
高强灌浆材料与带肋钢筋之间粘结性能的试验研究。*Construction and Building Materials*, 301:124059, （2021）。
[8] AZDINE I., KISSI B., KHATIB H.
钢—混凝土粘结连接件直接剪切行为研究。载于：*第二届应用科学、工程与技术创新国际会议（IRASET）论文集*，摩洛哥梅克内斯，页 1–4, （2022）。
[9] AZDINE I., KISSI B., KHATIB H., ZIRAOUI A.
钢与水泥灌浆界面剪切应力分析。*Materials Today: Proceedings*, （2025）。
[10] ILHAME A., BENAISSA K., HAMZA K., ADIL Z., MARIA E.
剪切力作用下水泥灌浆—钢板界面行为的试验研究。*Journal of Building Pathology and Rehabilitation*, 10, 52, （2025）。
[11] WILLIAMS PAUCHET.
钢—混凝土粘结性能。*Techniques de l'Ingénieur*, （2024）。
[12] ANTOINE TIXIER.
通过推入试验分析钢—混凝土界面行为：基于光纤测量与有限元建模。博士论文，格勒诺布尔大学, （2013）。
[13] ELIGEHAUSEN R., POPOV E. P., BERTERO V. V.
广义荷载作用下带肋钢筋的局部粘结应力–滑移关系。报告编号 UCB/EERC-83/23，1983 年 10 月。
[14] LIN H., ZHAO Y., OZBOLT J., FENG P., JIANG C., ELIGEHAUSEN R.
普通强度混凝土中带肋钢筋粘结应力–滑移关系的解析模型。*Construction and Building Materials*, 198:570–586, （2019）。

Manuscript Information
Word count: 9,312 words (excluding references).

Peer-Review Record
Fast-track status: Not fast-tracked.
First-round reviews received: 3 reports.
Revision cycles completed: 3 rounds.
Final version submitted: January 8, 2026